Available online at www.sciencedirect.com
SCIENCE DIRECT®
Acta Materialia 52 (2004) 2075–2080
Acta MATERIALIA
www.actamat-journals.com

Titanium's high-temperature elastic constants through the hcp–bcc phase transformation

Hirotsugu Ogi [a,*], Satoshi Kai [a], Hassel Ledbetter [b], Ryuichi Tarumi [a], Masahiko Hirao [a], Kazuki Takashima [c]

[a] Graduate School of Engineering Science, Osaka University, Machikaneyama 1–3, Toyonaka, Osaka 560-8531, Japan
[b] Los Alamos National Laboratory, M/S E536, Los Alamos, NM 87545, USA
[c] Precision and Intelligence Laboratory, Tokyo Institute of Technology, Yokohama, Kanagawa 226-8503, Japan

Received 14 November 2003; received in revised form 6 January 2004; accepted 7 January 2004

Abstract

The five independent elastic constants of hexagonal monocrystal titanium were determined up to the phase-transformation temperature, and the two isotropic elastic constants of polycrystalline titanium were determined beyond, up to 1300 K. Anomalous temperature dependences were observed just below the phase-transformation temperature: C_{11} and C_{66} increase with increasing temperature whereas C_{33} and C_{44} remarkably decrease, for example. To determine the C_{ij}, we used the free-vibration resonance frequencies obtained by electromagnetic acoustic resonance. After the phase transformation, the resonance frequencies changed little with the temperature increase, showing that the bcc-phase elastic constants change little with temperature. The polycrystalline elastic constants remained unchanged up to 1300 K after the phase transformation. The anomalous temperature dependence near the transformation is interpreted in terms of the small c/a ratio of the hcp phase and change of the atomic distances to meet the Burgers lattice relationship. Temperature-insensitive elastic constants in the bcc phase suggest the stabilizing of the bcc phase with increasing temperature.

Keywords: Elastic behavior; Strain ageing; Acoustic methods; Titanium; Martensitic phase transformation

1. Introduction

Titanium belongs to the group-IV metals, which show hcp (α)–bcc (β) phase transformation at temperatures higher than half the melting points. Elastic constants C_{ij} of titanium and its alloys received intensive study by Fisher and coauthors [1–3] who tried to clarify the transformation mechanism. They performed pulse-echo measurements independently for three specimens with different crystallographic orientations and determined the five elastic constants of hcp-phase titanium up to 1156 K for C_{11} and C_{44}, 1153 K for C_{66}, 1083 K for C_{33}, and 923 K for C_{13} [1]. Also, they used Ti–Cr binary-alloy specimens with different chromium concentrations to predict the unalloyed bcc-phase titanium C_{ij} using extrapolation [2,3]. However, the extrapolation is questionable because of rapid changes of elastic constants near the zero-chromium concentration. Thus, elastic constants of hcp-phase titanium just below the phase-transformation temperature and those of bcc-phase titanium remain uncertain and a central issue because of difficulties of high-temperature measurements.

Titanium exhibits an hcp lattice-parameter ratio c/a ($=1.59$) smaller than the ideal value ($=1.63$), indicating that its basal plane is dilated. Fisher and Renken [1] suggested that thermal-vibration modes would occur principally along the a-axis at low temperatures because of the elongated lattice and they would change to c-axis vibrations at the phase transformation to satisfy Burgers' relationship for the hcp–bcc phase transformation [4] and Zener's theory for high-temperature stability of bcc phases [5]. However, no study observed such effects near the phase transformation.

* Corresponding author. Tel.: +81-668-506-187; fax: +81-668-506-188.
E-mail address: ogi@me.es.osaka-u.ac.jp (H. Ogi).

1359-6454/$30.00 © 2004 Acta Materialia Inc. Published by Elsevier Ltd. All rights reserved.
doi:10.1016/j.actamat.2004.01.002

Here, we report measurements of the five hexagonal-symmetry elastic constants of monocrystal titanium up to the phase-transformation temperature and also the two isotropic elastic constants of polycrystalline titanium above the phase-transformation temperature. Elastic constants were determined simultaneously on a single specimen using electromagnetic acoustic resonance (EMAR). EMAR [6–9] is a noncontact method to measure free-vibration resonance frequencies of solids through the Lorentz-force or magnetostriction-force mechanism. The resonance frequencies are entered into an inverse calculation to determine all the independent elastic constants.

We observe elastic softening for C_{33} and C_{44}, and elastic stiffening for C_{11} and C_{66}, just below the phase-transformation temperature. Elastic softening is often observed near a phase transformation, but elastic stiffening seems unreported, thus presenting a new challenge for theory. Another important observation is the temperature-insensitive elastic constants of bcc-phase titanium.

2. Materials

Two specimens were prepared. One was a rectangular parallelepiped of monocrystal titanium, whose crystallographic axes were along the three sides. It was obtained by a strain-annealing technique: We applied a plastic deformation to a commercially available titanium rolled plate with 0.043-mass% oxygen content. The plate was heated to 1473 K with a rate 0.1 K/s and kept for 3 h in a pressure less than 10^{-5} Torr. It was cooled to 1123 K with a rate 7 K/s and kept for 24 h, and then furnace-cooled to room temperature. The procedure provided large grains with 15-mm diameter. We obtained the rectangular parallelepiped specimen from a single grain using the X-ray Laue method. The specimen measured 3.880 mm by 4.182 mm by 1.749 mm. The mass density was 4429 kg/m^3. The hexagonal-symmetry elastic constants are given by

$$[C_{ij}] = \begin{bmatrix} C_{11} & C_{12} & C_{13} & 0 & 0 & 0 \\ & C_{11} & C_{13} & 0 & 0 & 0 \\ & & C_{33} & 0 & 0 & 0 \\ & & & C_{44} & 0 & 0 \\ & \text{Sym.} & & & C_{44} & 0 \\ & & & & & C_{66} \end{bmatrix}. \quad (1)$$

Here $C_{66} = (C_{11} - C_{12})/2$.

The other specimen was a rectangular parallelepiped of a 99.96%-purity polycrystalline titanium, measuring 3.891 mm by 3.278 mm by 1.835 mm. The mass density was 4469 kg/m^3. Macroscopically, it shows two isotropic elastic constants, C_{11} and C_{44} (longitudinal modulus and shear modulus). We did not correct dimension and density changes caused by thermal expansion because the effect is small, comparable to the measurement errors.

3. Measurement

Fig. 1 shows our measurement setup. The specimen was inserted in a solenoid coil located within a cylindrical vacuum vessel made of austenitic-stainless steel. The solenoid coil was made with a Ni-alloy wire and its shape was held by a ceramic cement so as to operate at temperatures above 1300 K. A Cantal-line heater supplied the heat to the coil and specimen. The pressure inside the vessel was kept less than 10^{-4} Torr. A pair of permanent magnets made of Nd–Fe–B sintered material was set outside the vessel to apply a biasing magnetic field to excite and detect free vibrations of the specimen via the Lorentz-force mechanism. The permanent-magnet assembly was mounted on casters, which facilitated the rotation of field direction about the cylindrical-vessel axis and selection of detectable vibration modes. The detailed procedures for measuring resonance frequencies are given in a monograph by Hirao and Ogi [6].

There are eight vibration groups in free vibration of an oriented crystal with crystallographic symmetry higher than orthorhombic [10]. When the static field is along the coil's axial direction, breathing vibration (A_g group) appears. A static field perpendicular to the coil's axial direction causes shearing vibration (B_{1g}, B_{2g}, or B_{3g} group). (Notation of vibration group follows Mochizuki [11].) Thus, rotation of the permanent magnets allows one to excite one vibration group independently, leading to unambiguous mode identification, which is of great importance for the success of acoustic spectroscopicy. Here, we used A_g and B_{3g} vibrations. To determine the elastic constants, we performed an inverse calculation, the input being specimen mass, shape, and size, and measured resonance frequencies [10].

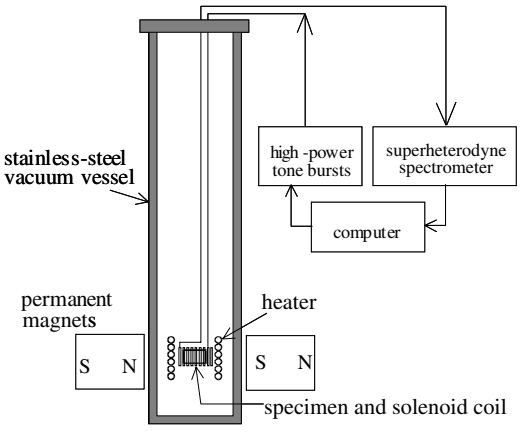

Fig. 1. Setup of high-temperature elastic-constant measurement by electromagnetic acoustic resonance.

4. Results

Fig. 2 shows changes of the resonance frequencies of the monocrystal specimen during heating. They decrease monotonically, but show anomalous changes just below the phase-transformation temperature. Upon heating, at the phase-transformation temperature, resonance peaks disappear, then another spectrum appears. Resonance frequencies of the bcc phase change little with temperature increase up to 1323 K.

Fig. 3 shows temperature dependences of principal hcp-phase elastic constants, including the results by Fisher and Renken [1] for comparison. B denotes the bulk modulus, and E_a and E_c denote Young's moduli along the a and c axes, respectively. The bcc-phase monocrystal elastic constants become unavailable because of transformation-induced twinning. At room temperature, we see elastic anisotropy between the directions parallel and normal to the basal plane: C_{11} smaller than C_{33} by 13%, E_a smaller than E_c by 41%, and C_{66} smaller than C_{44} by 32%. Significant behavior occurs just below the phase-transformation temperature as shown in Fig. 4: elastic constants related to the c-axis (C_{33}, E_c, and C_{44}) decrease, whereas those related to the a-axis (C_{11}, E_a, and C_{66}) increase.

Fig. 5 shows temperature dependence of the isotropic elastic constants of the polycrystalline specimen. Assuming that the material remained macroscopically isotropic after the hcp–bcc phase transformation, we determined the bcc-phase isotropic elastic constants. (This assumption was verified by two facts: the two elastic constants returned exactly to the initial values of the hcp phase at room temperature. The high-temperature-phase vibration spectrum fit well to assumed isotropic symmetry.) Fig. 5 also shows the effective (averaged-over-direction) constants calculated from the monocrystal-specimen values in Fig. 3 using the Voigt–Reuss–Hill averaging method. The polycrystalline-specimen elastic constants agree with the monocrystal-specimen elastic constants at room temperature,

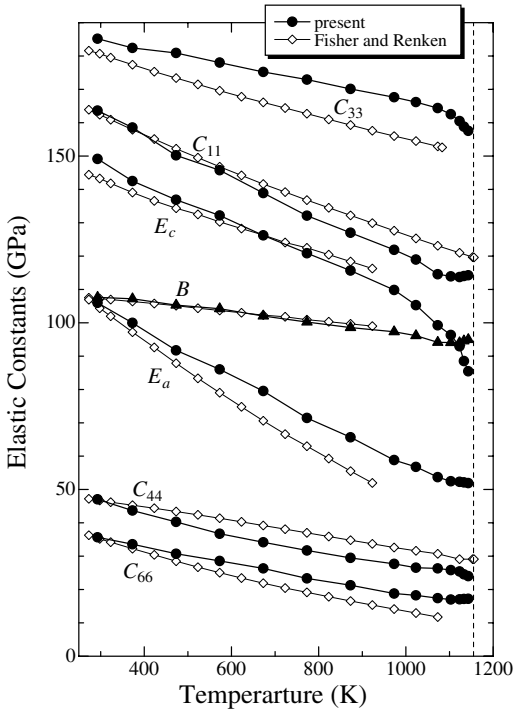

Fig. 3. Temperature dependences of monocrystal hcp-titanium elastic constants.

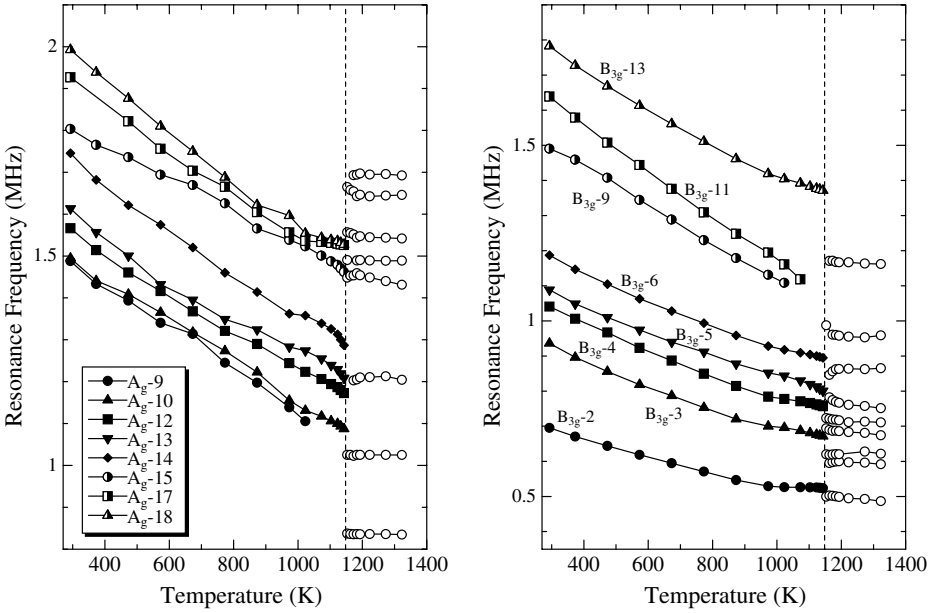

Fig. 2. Changes of resonance frequencies of A_g modes (left) and B_{3g} modes (right) with increasing temperature.

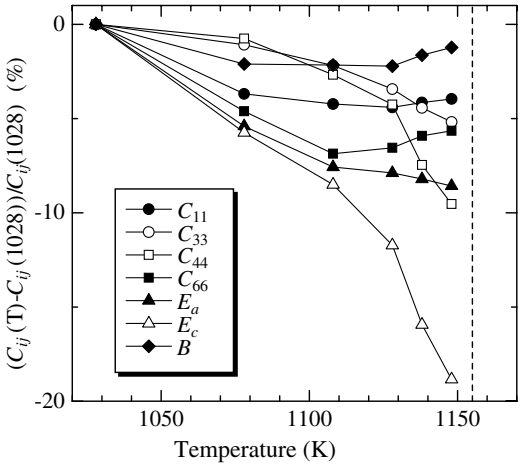

Fig. 4. Change of elastic constants of monocrystal hcp-titanium near the hcp-to-bcc phase-transformation temperature. Note both mode softening and mode stiffening. Largest changes occur in the c-axis Young modulus E_c. Smallest in the bulk modulus B.

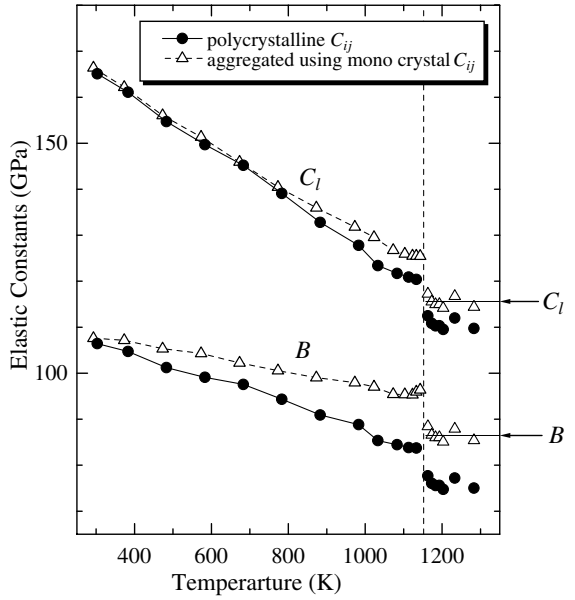

Fig. 5. Temperature dependences of elastic constants of polycrystalline titanium. B denotes bulk modulus and C_l longitudinal modulus. Open symbols show results calculated by the Voigt–Reuss–Hill averaging method using monocrystal elastic constants. The bcc-phase elastic constants are obtained by assuming the same polycrystal/monocrystal C_{ij} ratios in both phases.

but at high temperatures they fall below the monocrystal-specimen values.

5. Discussion

5.1. Hcp C_{ij} near the phase-transformation temperature

The lattice-parameter ratio c/a of hcp titanium is 1.59, smaller than the ideal value (1.63). This indicates larger atomic distance in the basal plane (0 0 0 1). This causes C_{66} to be smaller than C_{44}, C_{11} to be smaller than C_{33}, and E_a to be smaller than E_c. The normalized temperature derivatives $(1/C_{ij})\mathrm{d}C_{ij}/\mathrm{d}T$ of the elastic constants are larger for C_{66} than for C_{44}, and so on. This is also caused by the larger distance among the atoms constituting the (0 0 0 1) plane; a larger distance between atoms causes lower elastic stiffness and larger thermal vibration. Recent X-ray studies of titanium's anisotropic Debye–Waller factor B_{dw} support this view: Narayana et al. [12] gave the B_{dw} value along the a-axis larger than that along the c-axis by a factor 1.13. In a Debye model, the mean-squared atomic displacement varies as B_{dw}, which varies as reciprocal elastic-stiffness constant [13]. (Note that our C_{33}/C_{11} value at room temperature is also 1.13.) Because the c-axis thermal expansion exceeds the a-axis thermal expansion, high temperatures tend to reverse this anisotropy.

Approaching the transformation temperature at 1152 K, C_{11}, C_{66}, and E_a increase (Figs. 3 and 4), that is elastic stiffening approaching the transformation. This unusual stiffening can be attributed to premonitory behavior associated with the hcp–bcc Burgers mechanism [4]. The (0 0 0 1) closed-packed plane in the hcp phase becomes a (1 1 0) plane in the bcc phase. The lattice parameter in the hcp phase is $a = 2.95$ Å at room temperature [14]. That for the bcc phase is $a = 3.31$ Å at 1173 K, which means that the distance between nearest atoms is 2.86 Å [14]. Thus, the distance between the next-nearest atoms in the basal plane of the hcp phase decreases during the phase transition, which will increase C_{66}, C_{11}, and E_a. On the other hand, C_{33}, C_{44}, and E_c decrease just below the transformation, elastic softening. This supports the idea suggested by Fisher and Renken [1] that the direction of high-amplitude thermal vibration shifts from along the a-axis to the c-axis. The occurrence of the high-amplitude mode along the c-axis affects strongly the elastic constants C_{33}, C_{44}, and E_c so as to decrease them because of lattice anharmonicity.

5.2. Polycrystalline C_{ij} at high temperatures

Fig. 5 indicates elastic-constant softening at elevated temperatures in polycrystalline titanium. At 1123 K, the polycrystal/monocrystal elastic-constant ratios reach 0.87 for bulk modulus B and 0.96 for the longitudinal modulus C_l. Such elastic softening in a polycrystalline material is sometimes reported. For example, $B^{\mathrm{poly}}/B^{\mathrm{mono}} = 0.53$ and $C_l^{\mathrm{poly}}/C_l^{\mathrm{mono}} = 0.72$ for Nb_3Sn [15,16]. We attribute the present result to grain-boundary softening with two causes. First is mismatch of thermal-expansion coefficients along the a and c axes. As suggested by Fisher and Renken [1], titanium shows a marked positive temperature dependence of the c-axis thermal-expansion coefficient, which should increase the strain mismatch at the grain boundaries. A highly distorted structure near grain boundaries reduces elastic

stiffness. Second is impurity softening. Impurities such as oxygen tend to diffuse to grain-boundary sinks to form oxide layers, which reduce stiffness, especially at high temperatures.

We studied the influence of such an elastically softened region on the macroscopic elastic constants by a micromechanics calculation as shown in Appendix A. Our model is general; it should apply to any system where particles of one phase are enveloped by a softer-phase layer. The polycrystalline bulk modulus decreases by 0.91 and polycrystalline longitudinal modulus decreases by 0.93 compared with the non-defect material by the presence of very thin (aspect ratio $= 10^3$) and low-volume-fraction ($= 10^{-5}$) microcracks at grain boundaries. Thus, the elastic softening can be achieved by thin and soft inclusions on grain boundaries even when their volume fraction is quite small.

5.3. Bcc C_{ij}

The resonance frequencies in the bcc titanium show weak dependence on temperature. The normalized temperature derivative of the resonance frequency is about -3×10^{-4} K^{-1} in the hcp phase, whereas that in the bcc phase is of the order of 10^{-5} K^{-1}. Thus, the bcc-titanium elastic constants are essentially temperature-independent. We attribute this to structural stabilization with temperature increase; the bcc phase is unstable (softened) just above the transformation temperature. Further temperature increase decreases the instability, increases stiffness, offsetting the usual temperature-induced softening.

We determined bcc-phase elastic constants of the polycrystalline specimen using the measured resonance frequencies and mass density calculated from the lattice parameter at 1173 K [17]. However, because of the elastic softening of the polycrystalline specimen at higher temperatures, we corrected them assuming the same ratios of the polycrystalline C_{ij} to the aggregate C_{ij} from monocrystal C_{ij} both for the hcp and bcc phases. Thus determined bcc-phase elastic constants are $C_l = 115.3$ GPa, $G = 20.7$ GPa, and $B = 87.7$ GPa.

Table 1 compares our results with previous results: alloy-extrapolation results by Fisher and Dever [2] and force-constant neutron-scattering results from monocrystal measurements by Petry et al. [18]. (We averaged their values for monocrystal bcc-titanium to get the two quasi-isotropic elastic constants.) Our results agree well with those of Fisher and Dever. However, our results differ strongly from those of Petry et al.: our bulk modulus and longitudinal modulus are lower by 34% and 30%, respectively. Our bulk-modulus measurements on monocrystal hexagonal titanium give 96.4 GPa at 1143 K (Fig. 3), which agrees well with the Fisher and Renken value 99.7 GPa at 1146 K [1]. Thus, the Petry et al. results give a cubic/hexagonal bulk-modulus ratio of about 1.2, a 20% increase upon transforming to the cubic phase. Weston and Granato [19] measured the complete elastic-constant tensors for both phases of the hexagonal-cubic transformation in a cobalt–nickel alloy. They found a cubic/hexagonal bulk-modulus ratio of 0.90. A simple Einstein-oscillator model [20,21] also predicts a lower bulk modulus in the high-temperature phase. Furthermore, Nishitani et al. [22] obtained the bcc-titanium bulk modulus 107 GPa by first-principles calculations for zero temperature. Sanati et al. [23] also did the first-principles calculations and obtained 118 GPa for the zero-temperature bulk modulus. Their values would decrease by 10–20% at 1140 K, predicting a much smaller bulk modulus than that of Petry et al., thus supporting our result. We deduced the monocrystal bcc-titanium C_{ij}, which will be reported elsewhere [24].

Table 1
Elastic constants (GPa) of bcc polycrystalline titanium

	T (°C)	C_l	G	B	ν
Present	1000	115.3	20.7	87.7	0.391
Fisher and Dever [2]	1000	113.9	18.1	89.7	0.406
Petry et al. [18]	1020	149	23.2	118	0.408

C_l, G, B, and ν denote longitudinal modulus, bulk modulus, shear modulus, and Poisson ratio, respectively.

6. Summary

1. We determined the five independent elastic constants of monocrystal pure titanium up to the hcp–bcc phase-transformation temperature. Just before the transformation, the basal-plane-related elastic constants increase and c-axis-related elastic constants decrease remarkably. This can be explained by premonitory lattice deformation associated with the Burgers lattice correspondence in the hcp–bcc transformation.
2. The polycrystalline elastic constants soften at elevated temperatures, which we interpret as grain-boundary softening. We confirmed this with a micromechanics calculation.
3. We determined the polycrystalline elastic constants of bcc-phase titanium. They show almost no temperature dependence. They agree well with the Fisher–Dever estimate and disagree with the Petry et al. results. First-principles calculations support our results.

Appendix A. Micromechanics model for elastic softening in polycrystalline materials caused by grain-boundary softening

We represented the softened regions near grain boundaries with thin pancake-shape inclusions with smaller stiffness. The calculation contains two steps.

First, we calculate the five transverse-isotropic elastic constants of a composite consisting of isotropic titanium matrix including the inclusions whose minor axes are aligned along a particular direction. According to Eshelby's equivalent-inclusion theory [25] and Mori–Tanaka mean-field theory [26], such a two-phase composite elastic constants $\mathbf{C}_C$ are given by

$$\left.\begin{aligned}\mathbf{C}_C &= \mathbf{C}_M + [f_I(\mathbf{C}_I - \mathbf{C}_M)\mathbf{A}_d][f_M\mathbf{I} + f_I\mathbf{A}_d]^{-1},\\ \mathbf{A}_d &= [\mathbf{S}\mathbf{C}_\mathbf{M}^{-1}(\mathbf{C}_I - \mathbf{C}_M) + \mathbf{I}]^{-1}.\end{aligned}\right\}$$

Here $\mathbf{C}_M$ and $\mathbf{C}_I$ denote elastic constants of the matrix and inclusion, respectively, and $\mathbf{S}$ denotes Eshelby's tensor. f_M and f_I denote the volume fractions of the matrix and inclusion. Eshelby's tensor depends on the shape of inclusion and Poisson's ratio of the isotropic matrix. When the inclusions are ellipsoids, the nonzero components of $\mathbf{S}$ become simple and are tabulated in Mura's monograph [27]. Second, we calculate the effective (averaged-over-direction) elastic constants of the composite by averaging $\mathbf{C}_C$ using the Voigt–Reuss–Hill method. Thus, the resulting isotropic-symmetry elastic constants include the effect of randomly distributed thin inclusions. In the present study, we assumed microcracks on grain boundaries with an aspect ratio 10^3 and $f_I = 10^{-5}$.

References

[1] Fisher ES, Renken CJ. Phys Rev B 1964;135:A482.
[2] Fisher ES, Dever D. In: Jaffee R, Promisel NE, editors. The science, technology and application of titanium. New York: Pergamon; 1970. p. 373–81.
[3] Fisher ES, Dever D. Acta Metall 1970;18:265.
[4] Burgers WG. Physica 1934;1:561.
[5] Zener C. Elasticity and anelasticity of metals. Chicago: University of Chicago Press; 1948.
[6] Hirao M, Ogi H. EMATs for science and industry: noncontacting ultrasonic measurements. Boston: Kluwer Academic; 2003.
[7] Ogi H, Ledbetter H, Kim S, Hirao M. J Acoust Soc Am 1999;106:660.
[8] Ogi H, Ledbetter H, Takashima K, Shimoike G, Hirao M. Metal Mater Trans 2001;32A:425.
[9] Ogi H, Kai S, Ichitsubo T, Hirao M, Takashima K. Philos Mag A 2003;83:503.
[10] Ohno I. J Phys Earth 1976;24:355.
[11] Mochizuki E. J Phys Earth 1987;35:159.
[12] Narayana M, Kirishna N, Sirdeshmukh D. Acta Cryst A 2000;57:217.
[13] Grimrall G. Thermophysical properties of materials. Amsterdam: North-Holland; 1999 [Eqs. (7.44) and (7.47)].
[14] Pearson W. In: Handbook of lattice spacings and structures of metals and alloys, vol. 2. Oxford: Pregamon; 1967. p. 90.
[15] Keller K, Hanak J. Phys Rev 1967;154:628.
[16] Poirier M, Plamondon R, Cheeke J, Bussière J. J Appl Phys 1984;55:3327.
[17] Senkova ON, Chakoumakosb BC, Jonasc JJ, Froesd FH. Mater Res Bull 2001;36:1431.
[18] Petry W, Heiming A, Trampenau J, Alba M, Herzig C, Schober HR, et al. Phys Rev B 1991;43:10933.
[19] Weston W, Granato A. Phys Rev B 1975;12:5355.
[20] Grimrall G. Thermophysical properties of materials. Amsterdam: North-Holland; 1999. p. 116 [Eqs. (7.44) and (7.47)].
[21] Einstein A. Ann Phys 1911;34:170.
[22] Nishitani S, Kawabe H, Aoki M. Mater Sci Eng 2001;A312:77.
[23] Sanati M, Saxena A, Lookman T, Albers R. Phys Rev B 2001;63:224114.
[24] Ledbetter H, Ogi H, Kai S, Kim S, Hirao M. J Appl Phys 2004, in press.
[25] Eshelby JD. Proc Roy Soc Lond 1957;A241:376.
[26] Mori T, Tanaka K. Acta Metall 1973;21:571.
[27] Mura T. Micromechanics of defects in solids. 2nd ed. Dordrecht: Kluwer Academic; 1987.